Location of Shield Wires for Unconventional High Capacity Transmission Lines

Saikat Chowdhury, Babak Porkar, and Mona Ghassemi Zero Emission, Realization of Optimized Energy Systems (ZEROES) Laboratory Department of Electrical and Computer Engineering, The University of Texas at Dallas Richardson, TX, USA

Abstract— To achieve net-zero emission in America by 2050, high voltage transmission capacity must expand ~60% by 2030 and triple by 2050 to connect further wind and solar facilities to demand. This expansion requires a capital investment in transmission capacity of \$360 billion by 2030 and \$2.4 trillion by 2050. Considering the high cost of building transmission lines, innovations toward high-capacity overhead lines have been targeted to reduce the number of transmission lines required. In our previous studies, we introduced unconventional high-capacity transmission lines. To realize these novel transmission lines, various aspects of line design should be studied, and this paper addresses determining the location and number of shield wires to protect these novel lines against lightning strikes. Lightninginduced overvoltage across line insulators is one of the key factors in power system outages. The design meets the shielding failure flashover rate (SFFOR) $\leq 0.05/100$ km-years for all three phases of the unconventional high-capacity transmission line. Brown-Whitehead equations were used to measure and analyze the striking distance for vertical strokes.

Keywords—Lightning, unconventional high-capacity transmission lines, shielding failure flashover rate (SFFOR), shield wires, transmission lines.

I. INTRODUCTION

Lightning is one of the primary causes of disruptions on overhead power lines. Device failures and system outages brought on by lightning have been reported continuously [1-3]. To safeguard the networks, various strategies have been investigated so far in numerous studies [4]. Using shield wires/ground wires at the top of the tower can bring about substantial improvement in supporting the power conductors against lightning since it can safely conduct the high surge current to the ground when lightning strikes.

The shielding performance of the overhead lines lies in the optimal placement of the shield wires with respect to the phase conductors. The shield wires should be placed in such a way that the shielding failure flashover rate (SFFOR) is obtained at a minimal value. In practice to serve critical loads the acceptable SFFOR is within 0.05/100km-years [1]. Shielding analysis is contingent upon many parameters including length of the line and lightning strike density [1]. Electromagnetic models are adopted mostly to analyze the shielding performance of the transmission lines [5] where striking distance is used as a basic shielding analysis parameter [6-8]. For accurate prediction of striking distance, lightning parameters were discussed in [9]. By taking striking distance as the primary parameter, lightning

stroke model was designed for EHV and UHV transmission lines [10-12]. A different approach for evaluating shielding effectiveness is to use simulations taking upward leader inception as parameters [13-15]. To find the shielding failure probability, a numerical analysis based on electromagnetic field theory was discussed in [16]. In [17] a leader progression model was developed to assess shielding efficiency. More improvement in the leader progression model was developed in [18] where a 3D leader progression model was proposed in [19] and an algorithm was adopted to find out the shielding failure rate. This leader progression model was also used in [20] and applied to 500 kV overhead transmission lines.

In our previous study, a 500 kV unconventional highcapacity transmission line was proposed for the first time in [21]. Unconventional high-capacity transmission lines, distinguished by their non-traditional conductor arrangements and optimized phase configurations, offer a viable solution to meet the continuously increasing transmission capacity requirement, approximately 60% increase by 2030 and triple by 2050 in the US [6]. Moreover, due to the proliferation of renewable energy like wind farms and solar power plants, increasing transmission line capacity is becoming more crucial since most of the renewable farms are far from the load centers. Thus, more transmission lines will be required for power transmission. However, the cost of building new transmission lines is high, currently \$3.9M per mile to \$4.8M per mile in different states of the US [22]. As a result, designing a high-capacity transmission line like that introduced in [21] that delivers more power can result in fewer transmission lines required for power system planning, leading to remarkable savings.

II. THEORY AND METHODOLOGY

A. Lightning Mechanism

According to the stroke mechanism theory of lightning, a stepper leader moves forward the ground at the time of lightning and makes an upward conductive channel to flow the huge lightning current into the earth. This negative downward stroke/flash is the primary reason for most lightning incidents. The distance from the leader tip to any grounded structure is known as the striking distance which is highly dependent on the electric field and charge distribution on the stepped leader channel. Generally, in the analysis of shielding performance, two striking distances are considered, one is to the phase conductor or shield wires (r_c) and another is to the earth or

This work was supported in part by the National Science Foundation (NSF) under Award #2306098.

ground (r_g) . The expression of the striking distance is $r = AI^b$. The values of A and b have been estimated in many ways in different research studies. However, Brown and Whitehead equations are used mostly in lightning studies, and according to the Brown and Whitehead equation for vertical strokes, the values of A and b are listed in Table I.

TABLE I. PARAMETER VALUES FOR BROWN AND WHITEHEAD EQUATIONS

For r_g		For r_c		
Α	b	Α	b	
6.4	0.75	7.1	0.75	

B. Base Case

Fig. 1 shows the actual conventional 500 kV transmission line having 4 subconductors placed symmetrically on a circle in each phase [23]. But it has a low surge impedance loading (SIL), and thus to improve the SIL, we recently designed a 500 kV unconventional HSIL line [21] which is shown in Fig. 2 with 8 subconductors in each phase. Table II presents the positions of subconductors in our novel line shown in Fig. 2.

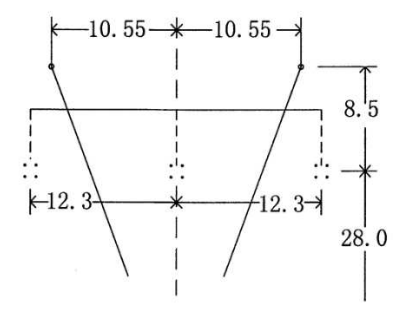


Fig. 1. 500 kV conventional transmission line.

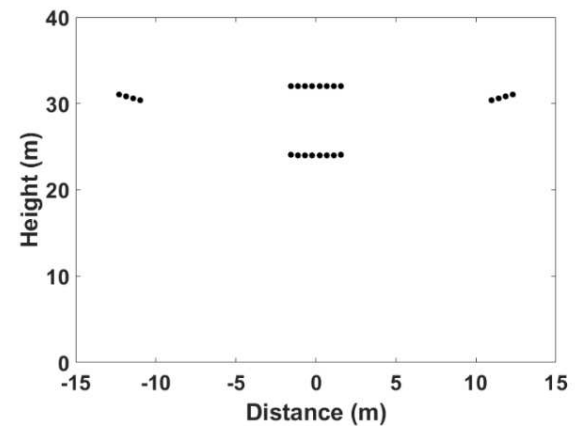


Fig. 2. The Unconventional HSIL line.

TABLE II. COORDINATES OF THE SUBCONDUCTORS

Phase A		Phase B		Phase C	
x (m)	y (m)	x (m)	y (m)	x (m)	y (m)
-1.5684	32.0492	-12.3	31.0258	-1.5684	24.0492
-1.1206	32.0251	-11.8547	30.8107	-1.1206	24.0251
-0.6729	32.009	-11.4069	30.6024	-0.6729	24.009
-0.2251	32.001	-10.9592	30.4021	-0.2251	24.001
0.2227	32.001	10.9567	30.401	0.2227	24.001
0.6704	32.009	11.4045	30.6012	0.6704	24.009
1.1182	32.025	11.8522	30.8095	1.1182	24.025
1.5659	32.049	12.3	31.0258	1.5659	24.049

This unconventional HSIL line improves the SIL 1.74 times compared to the 500 kV conventional line. In this paper, we want to design shield wires for this line, Fig. 2, where the highest height of subconductors in phase A, phase B, and phase C from the ground are 32.04 m, 31.02 m, and 24 m, respectively.

C. Calculation Parameters

The position and number of the shield wires are evaluated using the stroke mechanisms and the results are analyzed by considering the SFR and SFFOR values [1]. The shielding failure rate (SFR) is defined as the number of strokes that terminate on the phase conductor per 100 per year. SFR is expressed as

$$SFR = 2N_g L \int_2^{l_m} D_c f(I) dI$$
 (1)

where N_g represents ground flash density, L (km) represents the length of the line, D_c (km) represents the exposure distance for the phase conductor, I_m (kA) represents maximum current at and above which no stroke will be incident on the phase conductor. 3 kA is the lowest stroke current [1], and f(I) represents the probability density function of the occurrence of lightning current.

But not all the strokes are responsible for flashovers. Flashover occurs when the voltage induced by a stroke on the conductor exceeds the minimum voltage leading to a flashover known as critical flashover (CFO). The number of strokes on the phase conductors that result in a flashover is known as the shielding failure flashover rate (SFFOR). To find the equation of SFFOR, we need to change the lower limit of the current integral since SFFOR will only require the current responsible for flashover. Thus, SFFOR can be expressed as follows:

SFFOR =
$$2N_g L \frac{D_{cc}}{2} \int_{I_c}^{I_m} f(I) dI$$

= $2N_g L \frac{D_{cc}}{2} P(I_c \le I \le I_m)$
= $2N_g L \frac{D_{cc}}{2} [F(I_m) - F(I_c)]$
= $2N_g L \frac{D_{cc}}{2} [Q(I_c) - Q(I_m)]$ (2)

where

$$Q(I) = 1 - F(I) \tag{3}$$

and I_c is the critical value for stroke current at or above which flashover will occur and can be expressed in terms of critical flashover voltage (CFO) in kV and surge impedance of the phase conductor, $Z_c(\Omega)$ as follows:

$$I_c = \frac{2(\text{CFO})}{Z_c} \tag{4}$$

As seen in the equation of SFR and SFFOR, both are dependent on the value of ground flash density (N_g) and probability density function of current f(I). Both are associated with the natural lightning activity on the line located at a particular region given by [1]:

$$N_q = 0.04T_d^{1.25} (5)$$

where T_d is the number of thunderstorms per year, also known as the keraunic level. f(I) can be calculated by

$$f(I) = \frac{1}{\sqrt{2\pi}\beta I} e^{-\frac{1}{2}\left[\frac{\ln(I/M)}{\beta}\right]^2} \tag{6}$$

where M represents the median and β is the log standard deviation. Based on the value of current, I, their values can be considered as follows in Table III [1]:

TABLE III. PARAMETERS FOR f(I)

I [kA]	М	β	
3 to 20	61.1	1.33	
Greater than 20	33.3	0.605	

D. Methodology

At first, the surge impedance of all phases was calculated using the following methodology:

- For the horizontal position (x), the positions of the conductors in all phases were calculated based on a quadratic equation.
- The positions of the subconductors within each phase were calculated based on the spacing between them.
- GMR (geometric mean radius) and GMD (geometric mean distance) were calculated between all subconductors in all phases.
- According to the value of GMR (geometric mean radius) and GMD (geometric mean distance), inductance and capacitance were calculated, and finally, surge impedance of the line was obtained.

And, the following parameters were used in our study:

- CFO = 605 (kV/m) × minimum striking distance (m) is the empirical formula used to compute CFO (critical flash over density) [1].
- The critical current, I_C, is computed using the CFO and surge impedance values.
- The minimum striking distance was selected as 11.2 ft, which is usual for 500 kV lines.
- Two values of the number of thunderstorms per year, T_d =5 and T_d = 30 were taken into consideration for ground flash density to cover both regions with low and almost high lightning activity. In general, a value of T_d =5 is suitable for places with low lightning activity, whereas a value of T_d =30 is suitable for locations with almost high lightning activity [1]

In this paper, the tower height was chosen based on the coordinates presented in Fig. 2 by using the following equation:

$$h_t = y_A + \frac{2}{3}S\tag{7}$$

where y_A represents the height of phase A, S is the sag of the ground wire assumed 11.25 m which is usual for 500 kV lines. Based on the tower height, other parameters related to the Brown-Whitehead model were calculated. The geometrical parameters (α, β) , shown in Fig. 3, were calculated for each phase based on the Brown-Whitehead equation. Then a nested

loop command was performed to evaluate the value of SFFOR of each phase over a range of α or shielding angle values and was stored in an array to plot the result for analysis. Fig. 3 represents the geometry of the shield wire along with one of the phase conductors that was used for our calculation in this study.

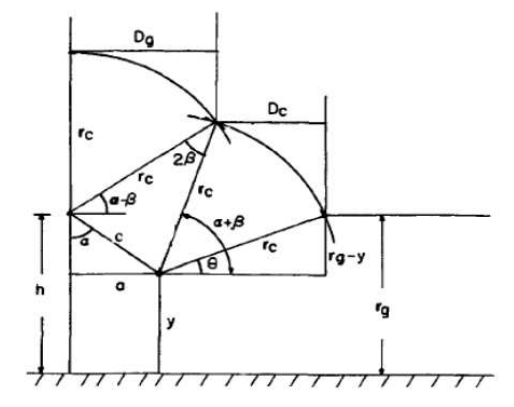


Fig. 3. Shield wire-phase conductor diagram.

From Fig. 3, h is the height of the tower that equals the height of the shield wire and y is the height of the phase conductor. The angle α as mentioned above is called the shielding angle. Our proposed methodology evaluates the position of shield wire based on the geometry of shielding angle. From the above geometry shown in Fig. 3

$$tan\alpha = \frac{a}{h - y} \tag{8}$$

From the plot of SFFOR flashovers/100 km-years vs shielding angle, the perfect shielding angle where the SFFOR meets the limit of 0.05 was determined. Then using Eq. (8), the position of the shield wire was obtained. The methodology is depicted in Fig. 4.

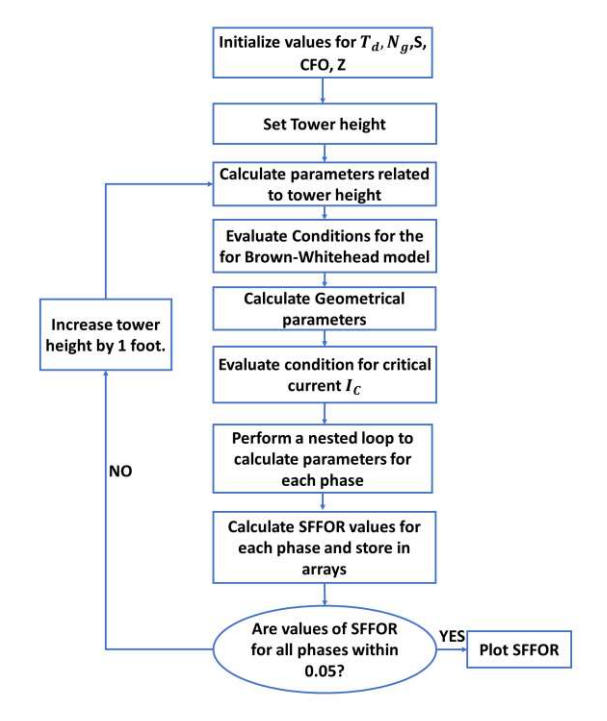


Fig. 4. Flowchart of the methodology to find SFFOR.

III. RESULTS AND ANALYSIS

Using the approach described above, the SFFOR for each of the three phases was plotted against the shielding angle for T_d =5 and T_d = 30 in Figs. 5 and 6, respectively.

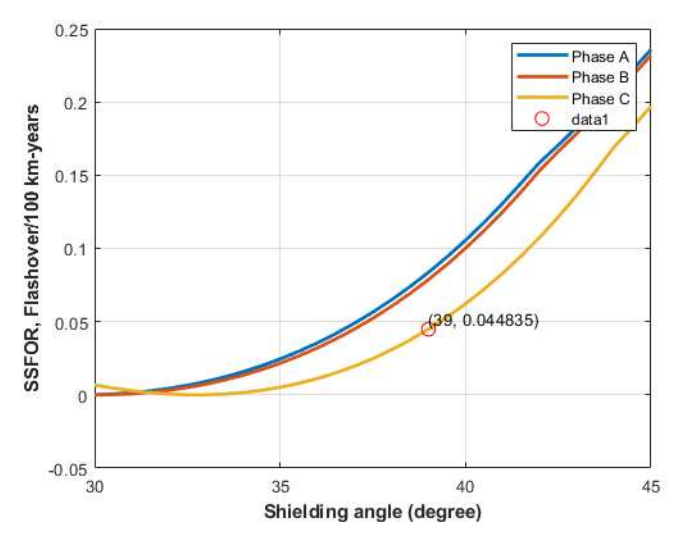


Fig. 5. SFFOR for different shield angles of the unconventional line for T_d =5.

From Fig. 5, to meet the SFFOR < 0.05 flashovers/100 km-years for all phases the shielding angle should be 39°. Thus, the distance between the shield wires, S_g , can be found using Eq. (8) as follows.

$$\tan 39^\circ = \frac{13.132 - S_g/2}{39.5 - 24.0492} \Rightarrow \frac{S_g}{2} = 0.62 \text{ m} \Rightarrow S_g = 1.24 \text{ m}$$

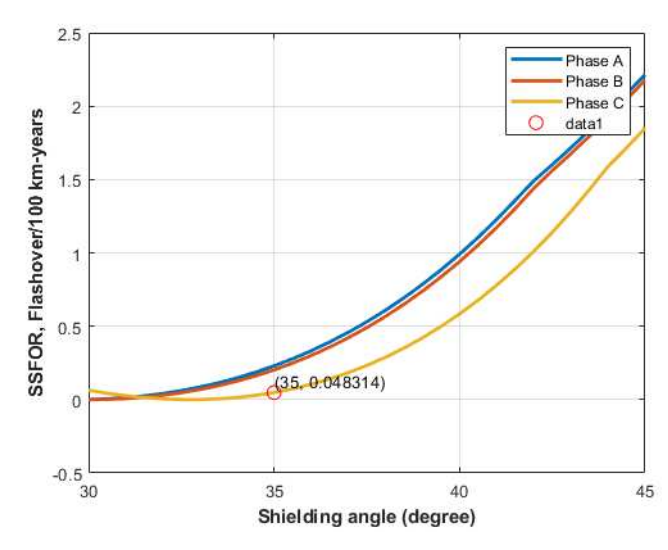


Fig. 6. SFFOR for different shield angles of the unconventional line for T_d =30.

From Fig. 6, to meet the SFFOR < 0.05 flashovers/100 km-years for all phases the shielding angle is 35° and the distance between the shield wires will be:

$$\tan 35^{\circ} = \frac{13.132 - S_g/2}{39.5 - 24.0492} \Rightarrow \frac{S_g}{2} = 2.31 \text{ m} \Rightarrow S_g = 4.62 \text{ m}$$

Figs. 7a and 7b show the location of shield wires for T_d =5 and T_d = 30, respectively.

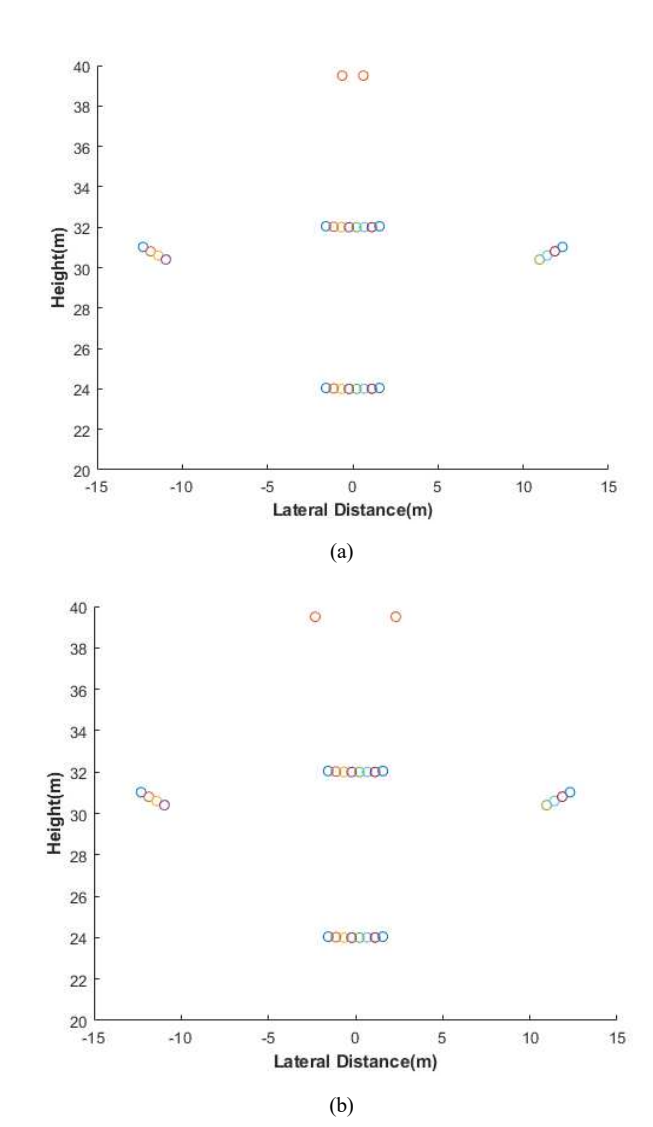
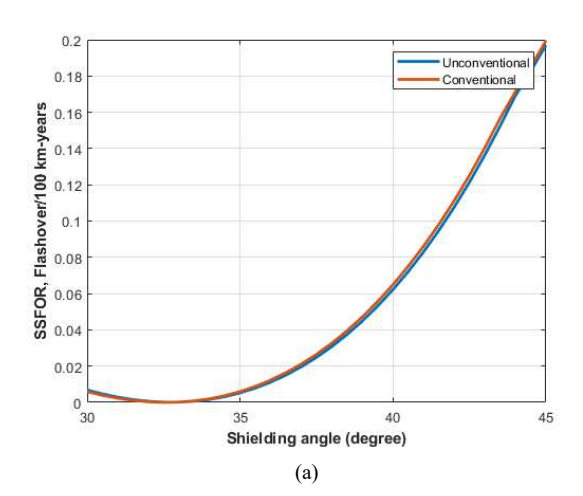


Fig. 7. Positions of shield wires along with subconductors for a) $T_d = 5$, and b) $T_d = 30$.

The SFFOR plots in Figs. 5 and 6, the dominant one, are compared in Fig. 8 with it for the conventional line shown in Fig. 1. As seen in Fig. 8, the SFFOR plots vs shielding angles are similar for both lines.



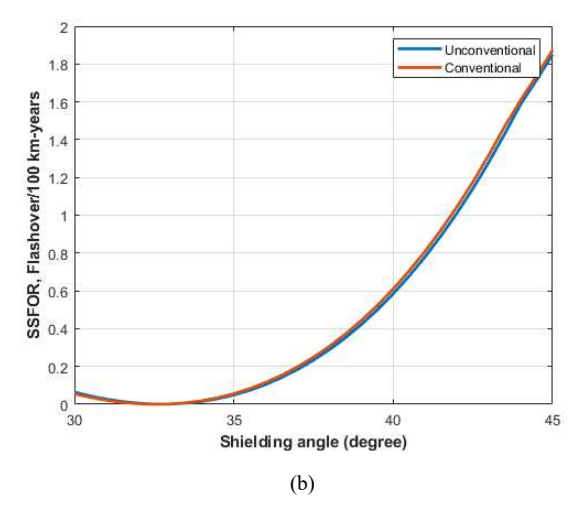


Fig. 8. SFFOR vs shielding angle for the conventional and unconventional lines for a) T_d =5, and b) for T_d =30.

In addition to different transmission line design aspects that need to be studied for unconventional lines having high-power delivery like those done in this paper and [24-26], live line working may be challenging due to the interaction of maintenance personnel and those lines with unconventional bundle arrangements, especially in freezing conditions [27-31].

IV. CONCLUSION

The paper calculates the number and location of shield wires for a new 500 kV unconventional high-capacity transmission line. In this regard, by calculating SFFOR for all three phases of the unconventional HSIL line, the exact location and number of ground wires were determined. The design of shield wires presented in this paper is an important step toward realizing unconventional HSIL lines that can revolutionize power delivery in future modern grids.

REFERENCES

- [1] IEEE Guide for improving the Lightning Performance of Transmission Lines, IEEE Std. 1243-1997, 1997.
- [2] E. Cinieri and F. Muzi, "Lightning induced overvoltages, improvement in quality of service in MV distribution lines by addition of shield wires," *IEEE Trans. Power Del.*, vol. 11, no. 1, pp. 361–372, Jan. 1996
- [3] J. Han et al., "Research on comprehensive protections of 10 kV overhead insulate distribution lines from lightning," *High Voltage Eng.*, vol. 34, no. 11, pp. 2395–2399, Nov. 2008
- [4] CIGRE-CIRED JWG C4.4.02: Protection of MV and LV networks against lightning. Part I: Common topics, Int. Council Large Electr. Syst. (CIGRE), Paris, France, CIGRE Tech. Brochure no. 287, 2006.
- [5] R. H. Golde, Lightning Protection, London U.K., Academic Press, Vol. 2, pp. 545-564, 1977.
- [6] F. S. Young, J. M. Clayton, and A. R. Hileman, "Shielding of transmission lines," *IEEE Trans. Power App. Syst.*, vol. S82, No. 4, pp. 132-154, 1963.
- [7] H. R. Armstrong and E. R. Whitehead, "Field and analytical studies of transmission line shielding," *IEEE Trans. Power App. Syst.*, vol. 87, pp. 270-281, 1968.
- [8] G. W. Brown and E. R. Whitehead, "Field and analytical studies of transmission line shielding-II," *IEEE Trans. Power App. Syst.*, vol. 88, pp. 617-626, 1969.
- [9] P. Chowdhuri and A. K. Kotapalli, "Significant parameters in estimating the striking distance of lightning strokes to overhead lines," *IEEE Trans. Power Del.*, vol. 4, pp.1970-1981, 1989.

- [10] D. W. Gilman and E. R. Whitehead, "The mechanism of lightning flashover on high-voltage and extra-high-voltage transmission lines", Electra, No. 27, pp. 65-96, 1973.
- [11] E. R. Whitehead, "CIGRE survey of the lightning performance of EHV transmission lines", Electra, No. 33, pp. 63-89, 1974.
- [12] L. D. Darveniza, F. Popolansky, and E. R. Whitehead, "Lightning protection of UHV lines", Electra, No. 41, pp. 39-69, 1975.
- [13] F. A. M. Rizk, "Modeling of transmission line exposure to direct lightning strokes", IEEE Trans. Power Del., Vol. 5, pp. 1983-1997, 1990
- [14] S. Ait-Amar and G. Berger, "A modified version of the rolling sphere method", IEEE Trans. Dielectr. Electr. Insul., Vol. 16, pp. 718-725, 2009
- [15] V. Cooray and M. Becerra, "Attractive radius and the volume of protection of vertical and horizontal conductors evaluated using a selfconsistent leader inception and propagation model – SLIM", 30th Int'l. Conf. Lightning Protection, Cagliari, Italy, paper No. 1062, 2010.
- [16] L. Dellera and E. Garbagnati, "Lightning stroke simulation by means of the leader progression model," *IEEE Trans. Power Del.*, vol. 5, pp. 2009-2029, 1990.
- [17] J. He, Y. Tu, R. Zeng, J. B. Lee, S. H. Chang, and Z. Guan, "Numeral analysis model for shielding failure of transmission line under lightning stroke," *IEEE Trans. Power Del.*, vol. 20, pp. 815-822, 2005.
- [18] B. Vahidi, M. Yahyaabadi, M. R. B. Tavakoli, and S. M. Ahadi, "Leader progression analysis model for shielding failure computation by using the charge simulation method," *IEEE Trans. Power Del.*, Vol. 23, pp. 2201-2206, 2008
- [19] B. Wei, Z. Fu, and H. Yuan "Analysis of lightning shielding failure for 500-kV overhead transmission lines based on an improved leader progression model," *IEEE Trans. Power Del.*, vol. 24, pp. 1433-1440, 2009.
- [20] M. R. B. Tavakoli and B. Vahidi, "Transmission-lines shielding failure rate calculation by means of 3-D leader progression models," *IEEE Trans. Power Del.*, vol. 26, pp. 507-516, 2011
- [21] M. A. Khan and M. Ghassemi, "A new unusual bundle and phase arrangement for transmission line to achieve higher natural power," *IEEE North American Power Symposium (NAPS)*, 2023, pp. 1-5.
- [22] MISO (Midcontinent Independent System Operator), Transmission Cost Estimation Guide For MTEP23, May 5, 2023
- [23] H. Wei-Gang, "Study on conductor configuration of 500-kV Chang-Fang compact line,", *IEEE Trans. Power Del.*, vol. 18, pp. 1002-1008, 2003.
 [24] M. A. Khan and M. Ghassemi, "Corona loss calculation for
- [24] M. A. Khan and M. Ghassemi, "Corona loss calculation for unconventional high surge impedance loading transmission lines," *IEEE North American Power Symposium (NAPS)*, 2023, pp. 1-6.
- [25] M. A. Khan and M. Ghassemi, "Calculation of audible noise and radio interference for unconventional high surge impedance loading (HSIL) transmission lines," *IEEE Conference Electrical Insulation Dielectric Phenomena (CEIDP)*, East Rutherford, NJ, USA, 2023, pp. 1-4.
- [26] M. A. Khan and M. Ghassemi, "A new method for calculating electric field intensity on subconductors in unconventional high voltage, high power density transmission lines," *IEEE Conf. Electrical Insulation Dielectric Phenomena (CEIDP)*, 2023, pp. 1-4.
- [27] M. Ghassemi, M. Farzaneh, and W. A. Chisholm, "Three-dimensional FEM electrical field calculation for FRP hot stick during EHV live-line work," *IEEE Trans. Dielectr. Electr. Insul.*, vol. 21, no. 6, pp. 2531– 2540, Dec. 2014.
- [28] M. Ghassemi, M. Farzaneh, and W. A. Chisholm, "A coupled computational fluid dynamics and heat transfer model for accurate estimation of temperature increase of an ice-covered FRP live-line tool," *IEEE Trans. Dielectr. Electr. Insul.*, vol. 21, no. 6, pp. 2628–2633, Dec. 2014.
- [29] M. Ghassemi and M. Farzaneh, "Coupled computational fluid dynamics and heat transfer modeling of the effects of wind speed and direction on temperature increase of an ice-covered FRP live-line tool," *IEEE Trans. Power Del.*, vol. 30, no. 5, pp. 2268–2275, Oct. 2015.
- [30] M. Ghassemi and M. Farzaneh, "Effects of tower, phase conductors and shield wires on electrical field around FRP hot stick during live-line work," *IEEE Trans. Dielectr. Electr. Insul.*, vol. 22, no. 6, pp. 3413– 3420, Dec. 2015.
- [31] M. Ghassemi and M. Farzaneh, "Calculation of minimum approach distances for tools for live working under freezing conditions," *IEEE Trans. Dielectr. Electr. Insul.*, vol. 23, no. 2, pp. 987–994, Apr. 2016.